Environmental Science Water Research & Technology

ROYAL SOCIETY OF CHEMISTRY

PAPER

View Article Online
View Journal | View Issue

Check for updates

Cite this: *Environ. Sci.: Water Res. Technol.*, 2020, **6**, 1058

Impact of transformation, photodegradation and interaction with glutaraldehyde on the acute toxicity of the biocide DBNPA in cooling tower water†

Thomas V. Wagner, *[ab] Rick Helmus, [a] Elmar Becker,[a] Huub H. M. Rijnaarts,[b] Pim de Voogt, [ab] Alette A. M. Langenhoff[b] and John R. Parsons[a]

Received 14th November 2019,
Accepted 5th February 2020

DOI: 10.1039/c9ew01018a

rsc.li/es-water

The reuse of cooling tower water (CTW) can substantially lower the freshwater footprint of cooling towers. CTW requires desalination before its reuse, and pre-treatment before desalination enhances the desalination efficiency. Constructed wetlands (CWs) have been shown to remove fractions from CTW that hamper physico-chemical desalination technologies, and thus provide adequate pre-treatment. However, CTW contains biocides, and these and their transformation products are potentially toxic to aquatic fauna in surface flow CWs. Therefore, we assessed the acute toxicity to daphnids of CTW which contained the biocide 2,2-dibromo-3-nitrilopropionamide (DBNPA), and the impact of photodegradation and the presence of biocide glutaraldehyde on its toxicity. It was observed that the toxicity of DBNPA in CTW was lower than that reported in the literature, and non-target screening showed that this was due to rapid DBNPA transformation, *via* 2-monobromo-3-nitrilopropionamide (MBNPA) and nitrilopropionamide (NPA). Photodegradation resulted in an increased CTW toxicity after 1 h of illumination as a result of the formation of new DBNPA transformation products, and subsequent decrease in toxicity after 48 h. The simultaneous presence of DBNPA and glutaraldehyde resulted in the formation of interaction products. Photodegradation did not result in unique interaction products, but increased the rate of interaction product formation, leading to a decrease in toxicity. Due to the toxicity of DBNPA in CTW and the effect of photodegradation on this toxicity, it is not recommended to use a surface flow CW as first treatment step in a multistage CW-system for the treatment of CTW.

Water impact

The reuse of discharged cooling tower significantly lowers the industrial fresh water footprint but requires desalination. A pre-treatment of the cooling tower water by constructed wetlands enhances the desalination efficiency. In this study, we determined the fate and toxic effect of biocides DBNPA and glutaraldehyde in cooling tower water in *Daphnia magna* that inhabit surface flow constructed wetlands.

1. Introduction

In industrialized areas around the globe, the fresh water uptake for cooling towers accounts for a significant part of the total industrial fresh water uptake.[1–3] After the cooling process, large volumes of cooling tower water (CTW) need to be discharged when the mineral concentration threshold is reached, for instance at an electric conductivity (EC) of >4500 μS cm^{-1}.[4] The reuse of brackish CTW after treatment in the cooling tower itself could significantly mitigate future fresh water scarcity problems.[3] CTW has to be desalinated prior to its reuse in the cooling tower.[4] However, physico-chemical desalination processes are hampered by CTW components, such as phosphate, nitrate and conditioning chemicals (CCs), that induce for instance fouling of reverse osmosis membranes.[5] To prevent technical problems, these fractions have to be removed prior to physico-chemical desalination. Constructed wetlands (CWs) are a sustainable

[a] *Institute for Biodiversity and Ecosystem Dynamics (IBED), University of Amsterdam, P.O. Box 94248, 1092 GE Amsterdam, The Netherlands*
[b] *Department of Environmental Technology, Wageningen University, P.O. Box 17, 6700 EV Wageningen, The Netherlands. E-mail: thomas.wagner@wur.nl, t.v.wagner@uva.nl; Tel: +31652654362*

† Electronic supplementary information (ESI) available. See DOI: 10.1039/c9ew01018a

pre-treatment option for the removal of these CTW fractions.[6]

CWs are man-made wetland systems that use natural removal processes, such as biodegradation, adsorption, plant uptake and photodegradation, for the removal of contaminants from waste water streams.[7–9] These biological, physical and chemical removal pathways occur simultaneously in CWs, and the contribution of each removal pathway to the total removal efficiency of a CW depends on the CW design. Adsorption and biodegradation are relevant removal pathways for conditioning chemicals from CTW in subsurface flow CW designs.[10,11] However, biodegradation of these chemicals by CW microorganisms is inhibited by the biocides 2,2-dibromo-3-nitrilopropionamide (DBNPA) and glutaraldehyde that are also present in CTW.[10] Furthermore, if DBNPA and glutaraldehyde are both present, they form interaction products as a result of mutual reactions, and these, in turn, decrease the toxicity of the biocides on the CW microorganisms.[10]

A potential way to mitigate the toxic effect of biocides on the biodegradation in a multistage CW is to remove them before the CTW enters the biologically active stages of a CW. This could be achieved by combining abiotic removal in a surface flow CW with biologically more active CW designs, such as vertical- and/or horizontal subsurface flow CWs. A potential abiotic removal pathway in surface flow CWs is photodegradation.[12–14] Photodegradation is the alteration of a chemical structure as a result of the exposure to sunlight. In the aquatic environment, both direct and indirect photodegradation occur. During direct photodegradation, the adsorption of sunlight results in a higher energy state and subsequent transformation of a chemical.[15,16] Indirect photodegradation is the alteration of a chemical as a result of the reaction with photochemically excited photosensitizers present in the aquatic system, such as hydroxyl radicals ($^{\bullet}OH$), singlet oxygen ($^1O_2$) and triplet excited dissolved organic matter (^3DOM).[13,16]

The commonly used biocide DBNPA is known to be susceptible to photodegradation,[17,18] and could potentially be removed from CTW in surface-flow CWs. Surface-flow CWs most closely resemble natural wetlands systems and are home to different aqueous and avian animal species. However, DBNPA photodegradation in surface-flow CWs could result in the production of various toxic transformation products.[17] Hence, the objective of the present research is threefold: i) to identify whether the discharge of CTW containing DBNPA is toxic to organisms that live in surface flow CWs used for the treatment of CTW, such as *Daphnia magna* ii) to determine whether photodegradation of DBNPA in surface flow CWs affects the DBNPA toxicity to *D. magna* iii) to determine whether DBNPA photodegradation result in unique DBNPA transformation products (TPs) and interaction products formed between glutaraldehyde and DBNPA in CTW,[10] and whether this has an influence on their combined toxicity to *D. magna* living in surface-flow CWs.

2. Materials & methods

2.1. Chemicals

DBNPA, glutaraldehyde (25% in H_2O), methanol (UHPLC-grade), synthetic sea salt, $NaHCO_3$, $CaCl_2$, $NaSeO_3$, formic acid (100%) and acetic acid (100%) were obtained from Sigma-Aldrich (Zwijndrecht, The Netherlands). $NaNO_3$ (>99%), $CaCl_2$ (>94%), Na_2SO_4 (>99%), KH_2PO_4 (>99%), humic acid (sodium salt) (45–70%), benzoic acid (>99.5%) and benzotriazole (>99%) for the preparation of synthetic CTW were obtained from Carl Roth GmbH (Karlsruhe, Germany).

2.2. Photodegradation set-up

Photodegradation experiments were performed in 4 different aqueous solutions, with biocide concentrations that are representative for real CTW:[19]

• Synthetic CTW, composed of $NaNO_3$ (83 mg L^{-1}), $CaCl_2$ (830 mg L^{-1}), Na_2SO_4 (1660 mg L^{-1}), KH_2PO_4 (10 mg L^{-1}), humic acid (50 mg L^{-1}), benzoic acid (50 mg L^{-1}) and benzotriazole (1 mg L^{-1}) dissolved in tap water. Characteristics of the synthetic CTW are described in Wagner *et al.* (submitted).
• Synthetic CTW + DBNPA (2.5 mg L^{-1}).
• Synthetic CTW + glutaraldehyde (2.5 mg L^{-1}).
• Synthetic CTW + DBNPA (2.5 mg L^{-1}) and glutaraldehyde (2.5 mg L^{-1}).

The photodegradation experiments were performed in triplicate in cylindrical glass reactors with quartz glass covers to prevent evaporation. These reactors were filled with 25 ml of one of the 4 matrices, placed on a Variomag Telesystem (Thermo Scientific, Breda, The Netherlands) and stirred with a magnetic stirrer at 175 rpm. Sunlight was simulated with 4 35 W xenon lamps (Hella, Nieuwegein, The Netherlands) in a home-build aluminium construction. The wavelength intensity distribution of this lamps and solar light is provided in the supplementary info (ESI;† Fig. S1). Each photodegradation replicate had a corresponding dark control that was wrapped in aluminium foil. Samples for non-target analysis and toxicity analysis were taken after 1, 48 and 96 h.

2.3. Non-target screening for transformation and reaction products

The formation of transformation products of DBNPA and interaction products from the reaction between DBNPA and CTW, DBNPA and glutaraldehyde and DBNPA, glutaraldehyde and CTW was determined by non-target screening. Non-target screening was performed based on the procedures described by Wagner *et al.*[10] on the four different matrices described in section 2.2 and their corresponding dark controls after 1, 48 and 96 h of illumination.

2.3.1. Instrumentation. UHPLC-q-ToF-MS/MS analyses were performed on a Nexera UHPLC system (Shimadzu, Den Bosch, The Netherlands) coupled to a maXis 4G high resolution q-ToF-MS/MS upgraded with a HD collision cell and equipped with an ESI source (Bruker Daltonics, Wormer, The Netherlands). Liquid chromatography was performed by a slightly modified version of a method developed by Albergamo *et al.*[20] In short, chromatography of a 20 μl sample was performed with a core–shell Kinetex biphenyl column (100 × 2.1 mm, 2.6 μm particle size and 100 Å pore size) (Phenomenex, Utrecht, The Netherlands) and the mobile phase consisted of solution A: ultrapure water with acetic acid (0.05% v:v) and solution B: methanol. A flowrate of 0.2 ml min^{-1} was used with a 19-minute gradient elution method starting at 0% B which increased linear to 100% B between minute 1 and 12. It was maintained at 100% B for 6 min, after which it decreased to the initial 0% B in 1 min. The system was then allowed to re-equilibrate for 7 min before the next sample was injected. Prior to each injection, a 50 μM sodium acetate solution in H_2O : MeOH (1 : 1 v:v) was introduced automatically for recalibration of the system. The column oven was kept at 40 °C. Mass spectrometry was performed with positive and negative ESI in separate runs with a resolving power typically of 30.000–60.000 FWHM.

2.3.2. Data processing workflow. UHPLC-q-ToF-MS/MS data was processed for non-target screening in the R programming language[21] using an in-house developed R package 'patRoon'.[22] The full R-script that is generated as a result of using the 'patRoon' workflow (Text S1) is provided in the ESI.† Two different scripts were used, one for positive and one for negative ionization measurements. The 'patRoon' package provides a common interface to various software solutions that are typically used to implement workflows for mass spectrometry based non-target analysis. Further details about the different software tools can be found at https://github.com/rickhelmus/patRoon.

The workflow of 'patRoon' (Fig. S2†) starts with the import of UHPLC-q-ToF-MS/MS measurements. The analyses were converted to open MS data format mzML by DataAnalysis. Subsequently, the replicates were grouped according to the sample names in Table 2 and the blanks for blank subtraction were determined. Afterwards, features were extracted for each measurements with OpenMS using the FeatureFinderMetabo algorithm, aligned according to retention time using the MapAlignerPoseClustering algorithm and grouped using the FeatureLinkerUnlabeled algorithm. To clean up the data, an intensity threshold of 5000 was used, and the features intensity had to be at least five times as high

Table 1 DBNPA transformation products identified by non-target screening in the dark controls and illuminated test solutions (TP1-TP4) and in the illuminated samples only (TP5-TP14)

TP#[a]	*m/z* (ionization mode)	Detected adduct	RT[b] (min)	Name and molecular formula	*m/z* deviation (ppm)	Level[c]	Test solution[d]
1	162.9500 (+) 160.9338 (−)	$[M + H]^+$ $[M - H]^-$	2.8	2-monobromo-3-nitrilopropionamide (MBNPA) $C_3H_3BrN_2O$	—	1	1-DBNPA-C 1-DBNPA-L
2	258.8714 (+)	$[M + H]^+$	4.9	2,2-dibromopropanediamide $C_3H_4Br_2N_2O_2$	0.7	1	1-DBNPA-C 1-DBNPA-L
3	215.86482 (+) 213.85049 (−)	$[M + H]^+$ $[M - H]^-$	5.7	2,2-dibromoacetamide $C_2H_3Br_2NO$	1.2	1	48-DBNPA-C 48-DBNPA-L 96-DBNPA-C 96-DBNPA-L
4	460.5483 (+)	$[M + H]^+$	10.3	$C_{19}H_{37}N_7O_6$	−2.9	4	1-DBNPA-C
5	153.0043 (−)	$[M - H]^-$	7.7	$C_2N_7O_2$	1.4	4	1-DBNPA-L 48-DBNPA-L 96-DBNPA-L
6	162.9137 (−)	$[M - H]^-$	2.2	C_2HBrN2O2	1.7	4	1-DBNPA-L 48-DBNPA-L 96-DBNPA-L
7	186.0409 (−)	$[M - H]^-$	10.9	$C_8H_5N_5O$	0.4	4	1-DBNPA-L 48-DBNPA-L 96-DBNPA-L
8	148.0146 (−)	$[M - H]^-$	7.1	$C_6H_3N_3O_2$	2.7	4	48-DBNPA-L 96-DBNPA-L
9	169.0139 (−)	$[M - H]^-$	2.6	$C_7H_6O_5$	1.4	4	48-DBNPA-L 96-DBNPA-L
10	173.0239 (−)	$[M - H]^-$	10.3	$C_{10}H_6O_3$	−2.6	4	48-DBNPA-L 96-DBNPA-L
11 12	206.0666 (+)	$[M + H]^+$	8.3 8.6	$C_8H_7N_5O_2$	2.7	4	48-DBNPA-L 96-DBNPA-L
13	344.1688 (+)	$[M + H]^+$	5.7	$C_{12}H_{21}N_7O_5$	−3.1	4	48-DBNPA-L 96-DBNPA-L
14	170.0559 (+) 168.0411 (−)	$[M + H]^+$ $[M - H]^-$	6.1	$C_6H_7N_3O_3$	0.6	4	96-DBNPA-L

[a] Transformation product number. In the text, this number is followed by the mass. [b] Retention time. [c] Identification level according to Schymanski *et al.* (2014).[23] [d] Only the presence in test solutions with DBNPA is indicated. The number corresponds with the hours after which the test solutions were sampled. The -L samples correspond to illuminated test solutions, while the -C samples correspond to the dark controls.

Table 2 Products formed as a result of the interaction between DBNPA and glutaraldehyde

GIP#[a]	m/z (ionization)	Detected adduct	RT[b] (min)	Molecular formula	m/z deviation (ppm)	Level[c]	Test solution[d]
1	128.07079 (+)	$[M + H]^+$	5.1	$C_6H_9NO_2$	−3.1	5	1-mix-C 1-mix-L 48-mix-C 48-mix-L
2	181.06119 (−) 183.07633 (+)	$[M - H]^-$ $[M + H]^+$	7.2	$C_8H_{10}N_2O_3$	0.6 0.1	3	1-mix-C 1-mix-L 48-mix-C 48-mix-L 96-mix-C 96-mix-L
3	183.07678 (−) 185.09193 (+)	$[M - H]^-$ $[M + H]^+$	3.8	$C_8H_{12}N_2O_3$	−0.3 0.7	5	1-mix-C 1-mix-L 48-mix-C 48-mix-L 96-mix-C 96-mix-L
4	263.0777 (−) 265.0931 (+)	$[M - H]^-$ $[M + H]^+$	7.9	$C_{11}H_{12}N_4O_4$	1.6 0.7	3	1-mix-C 1-mix-L 48-mix-C 48-mix-L 96-mix-C 96-mix-L
5	385.20753 (−)	$[M - H]^-$	9.1	$C_{17}H_{30}N_4O_6$	3.4	5	1-mix-C
6	264.06206 (−)	$[M - H]^-$	6.5	$C_{11}H_{11}N_3O_5$	1.8	5	48-mix-C 48-mix-L 96-mix-C 96-mix-L

[a] Glutaraldehyde interaction product number. [b] Retention time. [c] Identification level according to Schymanski *et al.* (2014).[23] [d] The number corresponds with the hours after which the test solutions were sampled. The -L samples correspond to illuminated test solutions, while the -C samples correspond to the dark controls.

as the blanks. In addition, the feature had to be present in all the replicates of a sample. In the next step, MS and MS/MS data were extracted using mzR. An average *m/z* window of 0.005 Da was used for clustering ions from multiple spectra along the chromatographic peak to average spectra. The maximum chromatographic peak window used for spectrum averaging was 5 s of the retention time. This was combined with a required minimal peak intensity of 500. The 50 highest MS and MS/MS peaks were kept. A default *m/z* window of 8 Da was used to find MS/MS spectra of a precursor ion. With GenForm, the MS and MS/MS data was used to predict molecular formulas. The elements used for molecular formula calculation were limited to C, H, N, O, P and Br to limit the calculation of improbable formulas and save calculation time. Any formula for a certain feature group was supposed to be detected in >75% of the measurements and the number of postulated formulas was limited to the 10 with the highest ranking. Subsequently, MetFrag was used for compound identification. A relative mass deviation of 5 ppm and an absolute mass deviation of 0.002 Da were used as thresholds. Potential candidates with the elements Cl, I, F, S and were excluded. The potential candidates were retrieved from PubChem and scored according to their similarity in fragmentation to in-silico generated MS/MS spectra and MassBank of North America (MoNA, http://mona.fiehnlab.ucdavis.edu/) derived mass spectra. The 25 candidates with the highest score were reported and considered for further interpretation. The next step was the generation of components. Isotopologues, multiple ionization adducts and in-source fragmentation can lead to different features with different *m/z* belonging to the same compounds. RAMclustR was used to cluster potential features in components that are likely to be the same compound. The last step of the 'patRoon' script consisted of the generation of a report of the results in CSV, PDF and HTML formats. These reports were manually checked for relevant features that could be compounds formed as result of the degradation of DBNPA or the interaction between glutaraldehyde and DBNPA. Subsequently, an identification confidence level was assigned according to Schymanski *et al.*[23] This was done by examining MS/MS spectra, peak shape and intensity of extracted ion chromatograms in Data Analysis (Bruker Daltonics, Wormer, the Netherlands), excluding isotopologues, excluding adducts and, where possible, confirmation with standards.

2.4. Acute toxicity tests with *Daphnia magna*

2.4.1. Test organism and test set-up. *Daphnia magna* was chosen as test organism because it is a well-described and frequently used test organisms for ecotoxicity testing.[24,25] *D. magna* also plays a key role in food webs of the temperate region and is therefore important for a healthy surface flow CW system. *D. magna* were cultured in Aachener Daphnien medium (ADaM) medium,[26] composed of synthetic sea salt,

$CaCl_2$, $NaHCO_3$ and Na_2SeO_3 in ultra-pure water, which was continuously aerated. The *Daphnia magna* were fed with 2 algae species and yeast during culturing.

D. magna 48 h acute toxicity tests were conducted based on OECD guideline 202 (ref. 25) and protocols described in Hernandez-Leal *et al.*,[27] Waaijers *et al.*[28] and de Baat *et al.*[29] The tests were performed in a test volume of 1 ml in 24-well plates that were covered by aluminium foil to prevent further photodegradation. Five *D. magna* neonates younger than 48 h were introduced to the wells by disposable transfer pipette, and the number of *D. magna* that were mobile after 24 h and 48 h were counted. The mobility of the *D. magna* was expressed as the percentage of mobility of the experimental control, and tests were considered valid with >80% mobility in the experimental controls.

2.4.2. DBNPA EC_{50} determination in ADaM-medium and cooling tower water. The EC_{50} of DBNPA in CTW and ADaM-medium was determined using 6 different DBNPA concentrations: 0, 0.25, 0.50, 1.0, 2.5 and 5.0 mg L^{-1}. Four replicates per concentration were used. In preliminary testing, no acute toxicity of CTW to the *D. magna* was observed (data not shown), and thus CTW without spiked DBNPA functioned as control for the experiments in CTW. The pH, dissolved oxygen and temperature of the test solutions were measured, and are provided in the ESI† (Table S1). Due to the instability of DBNPA, it was not possible to determine actual DBNPA concentrations at the beginning and end of the test.

2.4.3. Impact of photodegradation on the toxicity. Samples of 1 ml from the photodegradation experiments (see section 2.2) were taken for *D. magna* 48 h acute toxicity testing according to the protocol described in section 2.4.1. Four toxicity test replicates were performed for the triplicate samples from the photodegradation experiment. The dark control of CTW test solutions from the photodegradation experiment functioned as experimental control for the toxicity experiments. The pH, dissolved oxygen and temperature of the test solutions were measured, and are provided in the ESI† (Table S2).

2.4.4. Data analysis. A concentration-response relationship and the EC_{50} of DBNPA in CTW and ADaM medium was determined by non-linear regression with a log-logistic model in SPSS[30] according to Haanstra *et al.*[31] using eqn (1):

$$y(x) = \frac{c}{1 + e^{b\left(\log_{10}x - \log_{10}a\right)}} \tag{1}$$

In this equation, $y(x)$ is the control-normalized mobility of the *D. magna* at a DBNPA concentration x (mg L^{-1}), a is the estimated EC_{50} (mg L^{-1}), b is the slope of the curve and c is the normalized control mobility, which equals 100%.

Treatment effects on the mobility of *D. magna* were analysed using a one-way analysis of variance (ANOVA) in SPSS.[30] First, the *D. magna* mobility data was arcsine-transformed. Non-transformed data is shown in the figures. The homogeneity of variance was tested, and since the variance was not homogeneous, a Games–Howell *post-hoc* test was used to elucidate significant differences between treatments ($p \leq 0.05$).

3. Results and discussion

3.1. DBNPA transformation in cooling tower water lowers the DBNPA toxicity

A 24 h LC_{50} experiment with reference toxicant $K_2Cr_2O_7$ was performed according to our test protocol, and the LC_{50} of $K_2Cr_2O_7$ for the *Daphnia magna* culture and test set-up used in this study was 0.8 mg L^{-1} (Fig. S3†), which is within the LC_{50} range of 0.6–2.1 mg L^{-1} as set by the OECD guidelines.[25] The EC_{50} of DBNPA in CTW was 1.13 mg L^{-1}, which is higher than the DBNPA EC_{50} of 0.85 mg L^{-1} in ADaM-medium, implying that DBNPA in CTW is less toxic than in ADaM-medium (Fig. 1). The DBNPA EC_{50} in CTW of 1.13 mg L^{-1} is also higher than the EC_{50} values reported in literature, that range from 0.54–1.05 mg L^{-1}.[32] We used non-target screening on the dark controls of the photodegradation experiments to elucidate the mechanisms behind the reduced toxicity of DBNPA in CTW in our study.

Surprisingly, DBNPA itself was not identified with non-target screening, while the current non-target screening workflow can identify DBNPA.[10] This can be an indication that DBNPA was transformed in CTW in between the addition of DBNPA, taking the sample after 1 h and UHPLC-q-ToF-MS/MS analysis of the sample within the following 6 h. Complete DBNPA transformation in the dark as a result of chemical degradation within hours has been observed earlier.[18] A high pH of 8 increased the DBNPA transformation rate,[18] and the pH of CTW of 7.9 in the dark controls is similar (Table S6†). Various transformation products (TPs) that corroborate this rapid transformation of DBNPA were identified by the non-target screening (Table 1).

Similarly to our earlier study,[10] transformation products TP1-MBNPA (Table 1; Text S2†) and TP2-2,2-dibromopropanediamide (Table 1; Text S3†) were identified. However, the peak intensity of these TPs (Fig. S4†) was >5 times lower than those observed in that earlier study,[10] although the starting concentration of the biocides in the present study was higher. In our previous study, MBNPA was produced over time.[10] However, in the present study TP1-MBNPA is only detected at t = 1 h, indicating that this compound is further transformed. Blanchard *et al.*[18] identified two competing DBNPA transformation pathways: one leading to nitrilopropionamide (NPA) *via* MBNPA and one leading to 2,2-dibromoacetamide *via* dibromoacetonitrile. Dibromoacetonitrile was also observed in DBNPA transformation studies by Sumner & Plata.[33] An overview of known DBNPA degradation pathways is provided in Fig. S5.†

Comparison with an analytical standard showed that dibromoacetonitrile could not be detected with our chromatographical method. TP3-2,2-dibromoacetamide was identified using a commercially available standard after 48 h and 96 h (Table 1; Text S4†). The presence of TP3-2,2-dibromoacetamide can be an indication that the DBNPA in

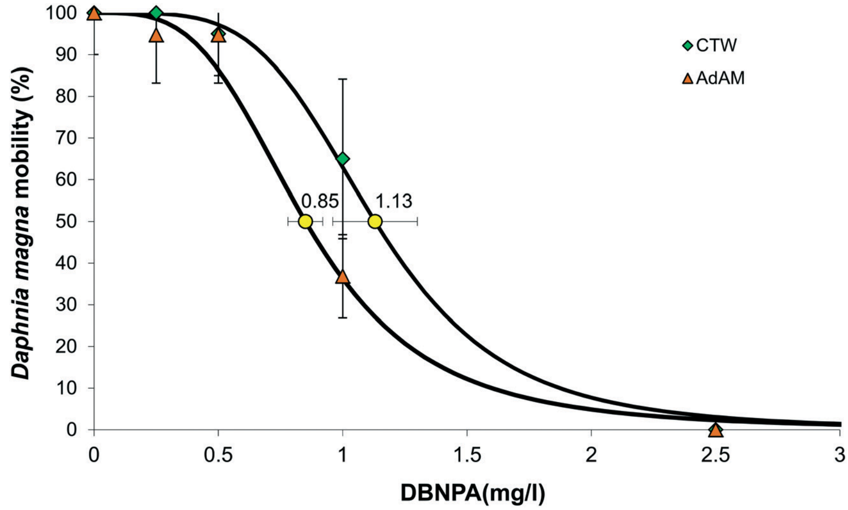

Fig. 1 The mobility of *Daphnia magna* after 48 h in the presence of different concentrations of DBNPA in ADaM medium (orange triangles) and cooling tower water (green diamonds), corresponding model fit (black lines) and EC_{50} (+95% confidence interval) for ADaM medium (yellow triangle) and cooling tower water (yellow diamond).

our CTW-matrix is transformed to dibromoacetonitrile and 2,2-dibromoacetamide within hours. This transformation to dibromoacetonitrile also explains the significant lower intensity of MBNPA than observed in our previous study,[10] where 2,2-dibromoacetamide was not observed at all.

In addition to known TPs of DBNPA, the previously unreported TP4-mz461 with a relatively high molecular mass of 460.5483 corresponding to $C_{19}H_{38}N_7O_6$ was detected (Table 1; Text S5†). This TP had a high peak intensity in comparison with the other DBNPA TPs (Fig. S4†). Both GenForm and MetFrag could explain the fragmentation of this TP (Text S5†), however a unique molecular structure could not be proposed by the latter software. The formation of TPs with a high mass, such as TP4-mz461, is either the result of the interaction of DBNPA with the CTW-matrix or the bimolecular reaction of DBNPA itself. DBNPA has been shown to produce tribromoacetonitrile and trihalogenated methanes as a result of bimolecular reactions.[17,33] The absence of bromine functional groups might be an indication that TP4-mz461 is indeed the result of the interaction of debrominated DBNPA TPs, either with each other or the CW-matrix. This could also be the reason that the peak intensity of TP1-MBNPA (Fig. S4†) is lower than that observed by Wagner *et al.*[10]

The toxicity of CTW containing 'DBNPA' will ultimately be determined by the toxicity of the mixture of DBNPA, TP1-MBNPA, TP2-dibromopropanediamide, TP3-2,2-dibromoacetamide, TP4-mz461 and potential TPs that were not identified, such as NPA or dibromoacetonitrile. The high peak intensity of TP4-mz461 in comparison with the other TPs (Fig. S4†) could be an indication that this TP contributes substantially to the lower than expected DBNPA toxicity to *D. magna*, if the toxicity of this compound is lower than DBNPA itself.

3.2. Impact of photodegradation on the acute toxicity of DBNPA

To test the applicability of surface-flow CWs for the photodegradation of DBNPA and the potential influence of photodegradation on the toxicity of DBNPA, photodegradation experiments with simulated sunlight and subsequent *D. magna* acute 48 h toxicity tests were performed. The toxicity of CTW containing DBNPA after 1 h of illumination is significantly higher than that of the dark control (Fig. 2), evidenced by the reduced *D. magna* mobility, implying that photodegradation increases the acute toxicity of DBNPA. The retention time of surface-flow CWs is higher than 1 h, and therefore the fauna in surface-flow CWs will be exposed to CTBD with an increased toxicity. This increase in toxicity cannot be attributed to changes in the CTW-matrix as a result of photodegradation, since illumination of the CTW-matrix did not result in a significant change of the *D. magna* mobility compared to the dark CTW-matrix control after 1 h (Fig. 2).

The non-target screening showed the presence of various products that were only detected in illuminated test solutions, confirming the previously described photodegradability of DBNPA.[17,34] These photodegradation products could not be identified, probably because the interaction between DBNPA and the CTW-matrix resulted in compounds that are not present in databases. However, a tentative molecular formula of these TPs could be determined. TP5-mz153 (Table 1; Text S6†), TP6-mz163 (Table 1; Text S7†) and TP7-mz186 (Table 1; Text S8†) were detected after 1 h, indicating that rapid formation of TPs occurred as result of photodegradation. After 48 h of photodegradation, new TPs were detected, such as TP8-mz148 (Table 1; Text S9†), TP9-mz169 (Table 1; Text S10†), TP10-mz173 (Table 1; Text S11†), TP11-mz206 and TP12-

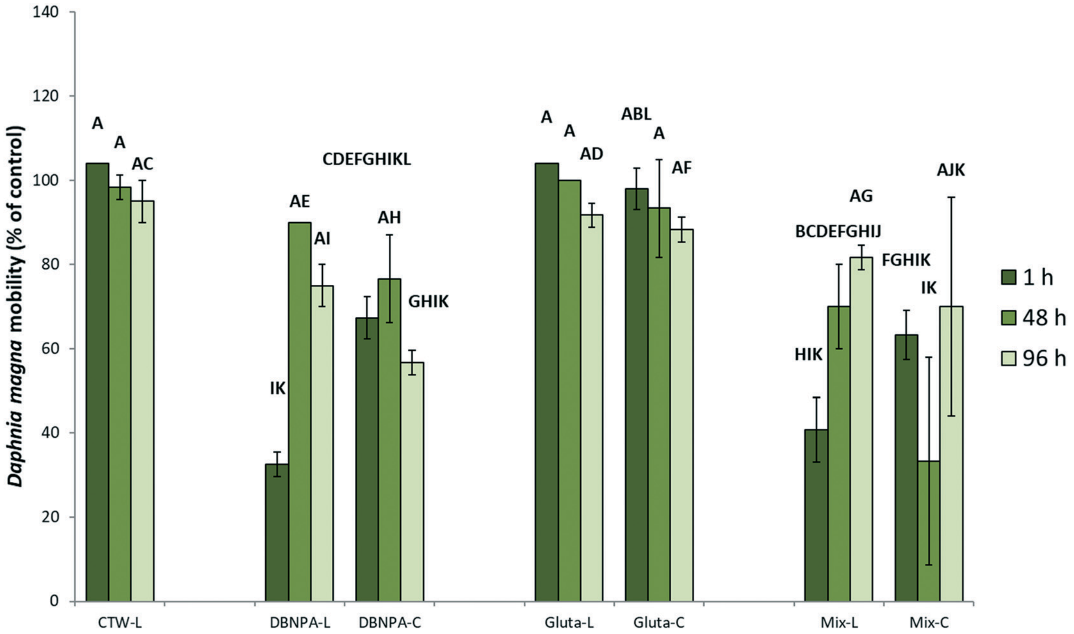

Fig. 2 Control-normalized mobility of *Daphnia magna* at t (h) 1, 48 and 96. CTW = synthetic cooling tower water; DBNPA = 2.5 mg L^{-1} DBNPA in synthetic cooling tower water; Gluta = 2.5 mg L^{-1} glutaraldehyde in synthetic cooling tower water; mix = 2.5 mg L^{-1} DBNPA + 2.5 mg L^{-1} glutaraldehyde in synthetic cooling tower water. The -L samples correspond to the illuminated test solutions, while the -C samples correspond to the dark controls. Different letters above bars indicate statistical differences (Games–Howell *post-hoc* test, α = 0.05).

mz206 (Table 1; Text S12†) and TP13-mz344 (Table 1; Text S13†). TP13-mz344 is another indication that new TPs with a larger *m*/*z* than DBNPA itself are formed. The formation of TP8-TP13 (Fig. 3B coincided with a decline in peak intensity of the TPs that already formed after 1 h (Fig. 3A), indicating possible transformation of TPs formed after 1 h to new TPs.

The TPs that were detected first after 48 h behaved differently; TP8-mz148 was detected with a high peak intensity compared to TP9-mz169 and TP13mz344 but decreased in peak intensity at 96 h (Fig. 3B). In contrast, TP9-mz169 and TP13-mz344 further increased in peak intensity at 96 h (Fig. 3B). At this time point, TP14-mz170 (Table 1; Text S14†) was first detected.

The non-significant difference in the toxicity after 1 h between illuminated DBNPA solutions and DBNPA dark controls is likely a result of the formation of

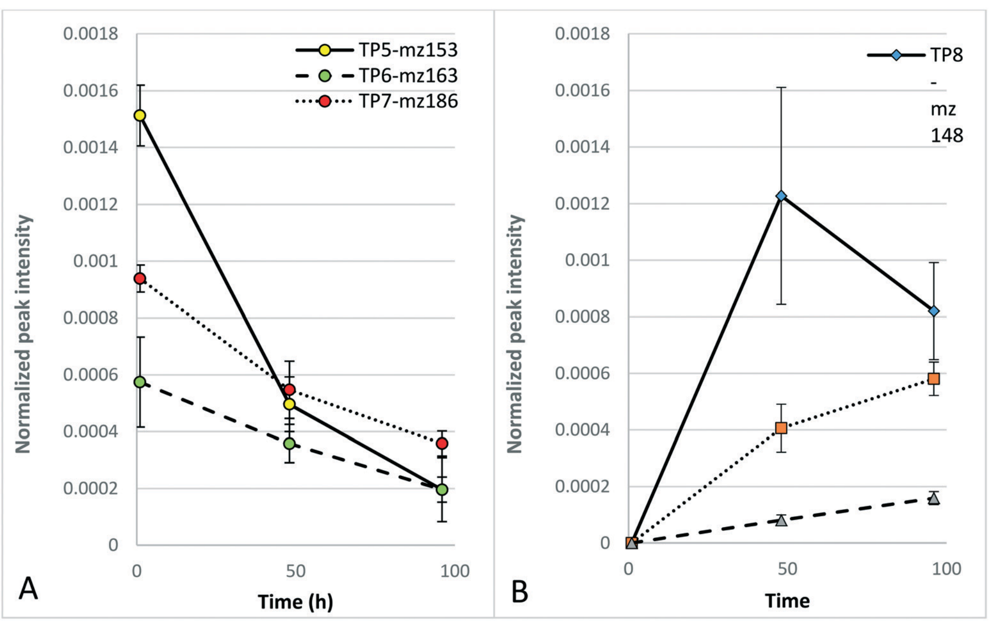

Fig. 3 Normalized peak intensities of TPs of DBNPA present in illuminated test solutions at t = 1 (A) and from t = 48 onwards (B). Peak areas are normalized based on the intensity of all extracted features per replicate.

photodegradation products that are more toxic than the products formed in the dark (section 3.1). In addition, TP4-mz461 was not present in the illuminated test solutions, while it was considered to be responsible for the reduced toxicity of DBNPA in CTW (section 3.1). The decrease in toxicity of the illuminated DBNPA test solutions after 48 h might coincide with the further photodegradation of the relatively toxic TPs initially formed after 1 h (Fig. 3A) and the formation of less toxic TPs between 1 h and 96 h (Fig. 3B).

3.3. Formation of glutaraldehyde interaction products in cooling tower water

To determine the influence of photodegradation on the formation of glutaraldehyde interaction products (GIPs) and their corresponding toxicity in CTW, non-target screening and *D. magna* acute 48 h toxicity tests were performed on CTW solutions in which both biocides were spiked.

3.3.1. The effect of glutaraldehyde interaction products on the toxicity of DBNPA in the dark. The presence of both biocides in the test solution does not result in a significantly different *D. magna* mobility compared to DBNPA only after 1 h for the dark controls (Fig. 2). The toxicity that was observed is not caused by glutaraldehyde, since the addition of 2.5 mg L^{-1} glutaraldehyde did not result in significant toxic effects compared to the CTW dark control (Fig. 2). The similar toxicity of the DBNPA solution and the DBNPA + glutaraldehyde solution is in contrast with the synergistic toxic effects of the mixture as observed by Ganzer *et al.*[35] In addition, the mixing of the two biocides in this study does not result in antagonistic toxic effects, as observed for CW microorganisms by Wagner *et al.*[10] The antagonistic toxic effects in the latter study were attributed to the formation of reaction products from the interaction between the two biocides and the interference of glutaraldehyde with the transformation of DBNPA.[10] It was already shown in section 3.1 that the transformation of DBNPA in CTW follows a different pathway to that observed by Wagner *et al.*[10] as result of the composition of the solution, which resulted in a DBNPA toxicity lower than observed previously. In addition, various tentative GIPs were detected in the present study.

GIP1 (Table 2; Text S15†), with a retention time of 5.1 min, was not observed in the Wagner study.[10] GIP1 could either be an interaction product between DBNPA and glutaraldehyde itself, or a fragment of a larger GIP. Four more GIPs with a higher *m*/*z* than that of GP1 were found, that were also observed by Wagner *et al.*[10] GIP2 (Table 2; Text S16†), GIP3 (Table 2; Text S17†), and GIP4 (Table 2; Text S18†) are likely to be the result of the interaction between glutaraldehyde and the debrominated DBNPA transformation product NPA.[10] In addition, TP13-mz344 (Table 1) was observed with a high peak intensity, and GIP5 (Table 2; Text S19†) could be an indication that reaction products were formed from the interaction between this TP and glutaraldehyde.

GIP2 was present with a substantially higher peak intensity (Fig. S6†) than in the study by Wagner *et al.*,[10] indicating that DBNPA must have been present and was transformed within hours. In addition, this might indicate that MBNPA is also quickly transformed to NPA, which would explain the low peak intensity and sole presence at timepoint t = 1 of MBNPA. Another indication that debromination occurred within hours was the absence of a brominated TP with *m*/*z* 280 that was observed in the study by Wagner *et al.*[10] This TP resulted from the interaction of MBNPA with glutaraldehyde,[10] and its absence in the present study corresponds with the substantially lower peak intensity of MBNPA (section 3.1). The peak intensity of GIP2 and absence of a GIP with *m*/*z* 280 provide evidence that DBNPA transformation *via* MBNPA and NPA is the most likely option of the two DBNPA transformation pathways discussed in section 3.1.

3.3.2. The impact of the transformation of glutaraldehyde interaction products on the acute toxicity. The mobility of *D. magna* exposed to the dark controls of CTW containing the glutaraldehyde and DBNPA mixture at 48 h decreased compared to the toxicity at 1 h (Fig. 2), indicating an increase in toxicity. A high variability in toxicity between the replicates was observed (Fig. 2), that could not be explained. Neither the solutions with only DBNPA nor with only glutaraldehyde experienced a similar increase in toxicity to *D. magna*. Hence, the increase in the DBNPA plus glutaraldehyde test solutions is likely the result of the toxicity of the GIPs formed.

Photodegradation resulted in a *D. magna* mobility in the DBNPA plus glutaraldehyde mixture that was not statistically different to the mobility in the illuminated DBNPA test solutions after 1 h (Fig. 2). This indicates that the toxicity of the mixture of biocides is mainly determined by the toxicity of the DBNPA photodegradation TPs (section 3.2). In contrast to the dark controls (section 3.3.2), photodegradation resulted in a significant decrease of the toxicity of the mixture of biocides between 1 h and 96 h (Fig. 2). This trend is also similar to the one observed in the illuminated DBNPA test solutions (Fig. 2).

Photodegradation did not result in the formation of unique reaction products formed as result of the interaction between DBNPA and glutaraldehyde in the light. Fig. 4 provides an overview of the TPs and GIPs of DBNPA that were identified in the various experimental setups of the present study. Photodegradation of DBNPA results in various TPs that are only formed in surface-flow CWs (Fig. 4). The interaction with glutaraldehyde results in the formation of GIPs, but none of these is formed exclusively as a result of photodegradation in surface flow CWs, and can thus also be formed in subsurface-flow CWs.

3.4. Implications of DBNPA photodegradation on cooling tower water treatment in full-scale constructed wetlands

The toxicity of biocide DBNPA in CTW to *D. magna* was assessed to evaluate the potential toxicity of DBNPA-containing CTW to fauna living in surface-flow CWs used for the treatment of CTW. DBNPA was less toxic to *D. magna* in

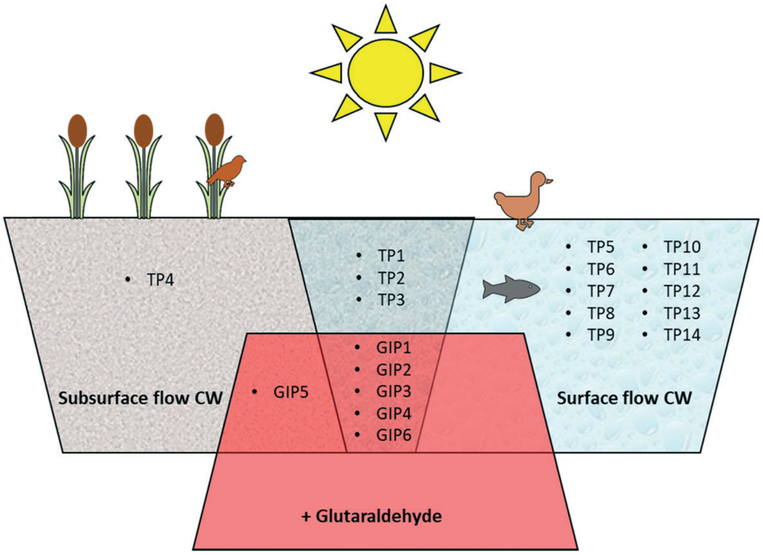

Fig. 4 Venn-diagram of transformation products of DBNPA in cooling tower water formed in the dark in subsurface-flow constructed wetlands, as a result of photodegradation in surface-flow constructed wetlands and as a result of the interaction with glutaraldehyde in either type of CW.

CTW than in ADaM medium. Non-target screening showed that this is likely due to the rapid transformation of DBNPA *via* the MBNPA–NPA pathway. Photodegradation of DBNPA in CTW resulted in the formation of various direct TPs of DBNPA that significantly increased the toxicity of the DBNPA mixture to *D. magna* after 1 h of illumination. This increased toxicity of CTW introduced into the CW can have detrimental effects on the fauna living in surface-flow CWs. To determine the impact of DBNPA on the fauna in surface flow CWs, it is recommended to test the effect of DBNPA in CTW on both aquatic species as well as birds and mammals. An overview of DBNPA 96 h LC_{50} and 24 h LC_{50} values for different aquatic species, such as different fish species, shrimp, oyster and crab, is provided by Klaine *et al.*,[32] and these values range from 0.3 mg L^{-1} to 14 mg L^{-1}. However, since the transformation of DBNPA has shown to be dependent on the water matrix composition by the present study as well as a previous one,[10] it is recommended to repeat these tests in genuine CTW to predict the impact on a full-scale surface flow CW.

In addition to aquatic fauna, avian fauna can enter surface flow CWs and be affected by toxic substances. In subacute dietary toxicity tests, DBNPA LC_{50} values of >10 000 mg L^{-1} for mallard ducks (*Anas platyrhynchos*) and >5620 mg L^{-1} for bobwhite quail (*Colinus virginianus*) were observed,[36] and thus no effect of DBNPA in CTW for avian species entering surface flow CWs can be expected because of the much lower actual concentrations of DBNPA in CTW.

The abovementioned studies determined the acute toxicity of DBNPA, which would resemble a single exposure event to DBNPA. However, biocides are generally continuously dosed to cooling systems to prevent microbial fouling.[3] Therefore, chronic toxicity studies with DBNPA in CTW are needed. Cheng[37] showed that chronic toxicity tests with DBNPA in mineral water resulted in lower 21 d EC_{50} values for *D. magna*, with 0.072 mg L^{-1} for longevity, 0.053 mg L^{-1} for reproduction and 0.055 mg L^{-1} for brood size. These values are substantially lower than the acute 48 h EC_{50} value for mobility observed in the present study (section 3.1). Nevertheless, it is common practice in cooling towers to shock-dose DBNPA, when the microbial fouling in the cooling system reaches a threshold value.[32] This results in short episodes of discharge of CTW with DBNPA into surface flow CWs. Hence the concentration of the mixture of toxic TPs of DBNPA will be diluted if residual DBNPA TPs from a previous shock-dose episode are removed in the CW, and thus the exposure to DBNPA TPs will be non-chronic.

In a preceding study,[38] we proposed a system of sequential CWs as a suitable pre-treatment option for CTW prior to desalination. However, the toxicity to aquatic fauna in surface-flow CWs was not assessed in the latter study. When a surface flow CWs is deemed necessary in a hybrid-CW system for the treatment of CTW, for instance for the storage of large volumes of CTW, the results from the present study suggest to not use the surface CW as a first treatment step in a hybrid-CW and to start the hybrid-CW with a subsurface flow to prevent unwanted toxic effects to aquatic fauna in subsequent surface flow CWs. DBNPA concentrations of 1 and 10 mg L^{-1} did not negatively affect the biodegradation in these subsurface-flow CWs. Furthermore, no detectable DBNPA concentrations were observed in the effluent of the subsurface-flow CWs,[38] and thus no DBNPA would enter a subsequent surface-flow CW.

Conflicts of interest

There are no conflicts of interest to declare.

Acknowledgements

This research is financed by the Netherlands Organisation for Scientific Research (NWO), which is partly funded by the

Ministry of Economic Affairs, and co-financed by the Netherlands Ministry of Infrastructure and Environment and partners of the Dutch Water Nexus consortium (Project nr. STW 14302 Water Nexus 3). Milo de Baat and Michiel Kraak are acknowledged for their help in designing the toxicity tests. Taymaz Azarno and Titus Rombouts are acknowledged for maintaining the *Daphnia magna* cultures. Samira Absalah is acknowledged for her analytical support. Vinnie de Wilde, Bert Willemsen, Joke Westerveld and Merijn Schuurmans are acknowledged for technical support.

References

1 J. Macknick, R. Newmark, G. Heath and K. C. Hallett, Operational water consumption and withdrawal factors for electricity generating technologies: a review of existing literature, *Environ. Res. Lett.*, 2012, **7**, 045802.

2 C. Zhang, L. Zhong, X. Fu, J. Wang and Z. Wu, Revealing water stress by the thermal power industry in China based on a high spatial resolution water withdrawal and consumption inventory, *Environ. Sci. Technol.*, 2016, **50**, 1642–1652.

3 S. Pan, S. W. Snyder, A. I. Packman, Y. J. Lin and P. Chiang, Cooling water use in thermoelectric power generation and its associated challenges for addressing water-energy nexus, *Water-Energy Nexus*, 2018, **1**, 26–41.

4 C. K. Groot, W. B. P. van den Broek, J. Loewenberg, N. Koeman-Stein, M. Heidekamp and W. de Schepper, Mild desalination of various raw water streams, *Water Sci. Technol.*, 2015, **72**, 371–376.

5 J. Löwenberg, J. A. Baum, Y. Zimmermann, C. Groot, W. van den Broek and T. Wintgens, Comparison of pre-treatment technologies towards improving reverse osmosis desalination of cooling tower blow down, *Desalination*, 2015, **357**, 140–149.

6 T. V. Wagner, J. R. Parsons, H. H. M. Rijnaarts, P. de Voogt and A. A. M. Langenhoff, A review on the removal of conditioning chemicals from cooling tower water in constructed wetlands, *Crit. Rev. Environ. Sci. Technol.*, 2018, **48**, 1094–1125.

7 G. Imfeld, M. Braeckevelt, P. Kuschk and H. H. Richnow, Monitoring and assessing processes of organic chemicals removal in constructed wetlands, *Chemosphere*, 2009, **74**, 349–362.

8 J. Garcia, D. P. L. Rousseau, J. Morato, E. Lesage, V. Matamoros and J. M. Bayona, Contaminant removal processes in subsurface-flow constructed wetlands: A review, *Crit. Rev. Environ. Sci. Technol.*, 2009, **40**, 561–661.

9 Y. He, N. B. Sutton, Y. Lei, H. H. M. Rijnaarts and A. A. M. Langenhoff, Fate and distribution of pharmaceutically active compounds in mesocosm constructed wetlands, *J. Hazard. Mater.*, 2018, **357**, 198–206.

10 T. V. Wagner, R. Helmus, S. Quiton Tapia, J. R. Parsons, P. de Voogt, H. H. M. Rijnaarts and A. A. M. Langenhoff, Non-target screening reveals the mechanisms responsible for the antagonistic inhibiting effect of the biocides DBNPA and glutaraldehyde on benzoic acid biodegradation, *J. Hazard. Mater.*, 2020, **386**, 121661.

11 T. V. Wagner, J. R. Parsons, H. H. M. Rijnaarts, P. de Voogt and A. A. M. Langenhoff, Benzotriazole removal mechanisms in pilot-scale constructed wetlands treating cooling tower water, *J. Hazard. Mater.*, 2020, **384**, 121314.

12 J. T. Jasper and D. L. Sedlak, Phototransformation of wastewater-derived trace organic contaminants in open-water unit process treatment wetlands, *Environ. Sci. Technol.*, 2013, **47**, 10781–10790.

13 C. Prasse, J. Wenk, J. T. Jasper, T. A. Ternes and D. L. Sedlak, Co-occurence of photochemical and microbiological transformation processes in open-water unit process wetlands, *Environ. Sci. Technol.*, 2015, **49**, 14136–14145.

14 Y. He, N. B. Sutton, H. H. M. Rijnaarts and A. A. M. Langenhoff, Degradation of pharmaceuticals in wastewater using immobilized TiO_2 photocatalysis under simulated solar irradiation, *Appl. Catal., B*, 2016, **182**, 132–141.

15 E. De Laurentiis, C. Prasse, T. A. Ternes, M. Minella, V. Maurino, C. Minero, M. Sarakha, M. Brigante and D. Vione, Assessing the photochemical transformation pathways of acetaminophen relevant to surface waters: Transformation kinetics, intermediates and modelling, *Water Res.*, 2014, **53**, 235–248.

16 L. C. Bodhipaksha, C. M. Sharpless, Y. Chin and A. A. Mackay, Role of effluent organic matter in the photochemical degradation of compounds of wastewater origin, *Water Res.*, 2017, **110**, 170–179.

17 J. H. Exner, G. A. Burk and D. Kyriacou, Rates and products of decomposition of 2,2-dibromo-3-nitrilopropionamide, *J. Agric. Food Chem.*, 1973, **21**, 838–842.

18 F. A. Blanchard, S. J. Gonsoir and D. L. Hopkins, 2,2-dibromo-3-nitrilopropionamide (DBNPA) chemical degradation in natural waters: Experimental evaluation and modeling of competitive pathways, *Water Res.*, 1987, **21**, 801–807.

19 D. Benelux, personal communication, 2019.

20 V. Albergamo, R. Helmus and P. de Voogt, Direct injection analysis of polar micropollutants in natural drinking water sources with biphenyl liquid chromatography coupled to high-resolution time-of-flight mass spectrometry, *J. Chromatogr. A*, 2018, **1569**, 53–61.

21 R Core Team, *R: A language and environment for statistical computing*, R Foundation for Statistical Computing, Vienna, Austria, 2013, http://www.R-project.org/.

22 R. Helmus, *patRoon*, 2018, http://github.com/rhelmus.

23 E. L. Schymanski, J. Jeon, R. Gulde, K. Fenner, M. Ruff, H. P. Singer and J. Hollender, Identifying small molecules via high resolution mass spectrometry: Communicating confidence, *Environ. Sci. Technol.*, 2014, **48**, 2097–2098.

24 D. M. M. Adema, Daphnia magna as a test animal in acute and chronic toxicity tests, *Hydrobiologia*, 1978, **59**, 125–134.

25 Organisation for Economic Co-operation and Development (OECD), *OECD guideline for testing of chemicals – Daphnia sp., acute immobilisation test 202*, 2004.

26 B. Klüttgen, U. Dülmer, M. Engels and H. T. Ratte, ADaM, an artificial freshwater for the culture of zooplankton, *Water Res.*, 1994, **28**, 743–746.

27 L. Hernandez Leal, A. M. Soeter, S. A. E. Kools, M. H. S. Kraak, J. R. Parsons, H. Temmink, G. Zeeman and C. J. N. Buisman, Ecotoxicological assessment of grey water treatment systems with *Daphnia magna* and *Chironomus riparius*, *Water Res.*, 2012, **46**, 1038–1044.

28 S. L. Waaijers, J. Hartmann, A. M. Soeter, R. Helmus, S. A. E. Kools, P. de Voogt, W. Admiraal, J. R. Parsons and M. H. S. Kraak, Toxicity of new generation flame retardants to *Daphnia magna*, *Sci. Total Environ.*, 2013, **463–464**, 1042–1048.

29 M. L. de Baat, M. H. S. Kraak, R. van der Oost, P. de Voogt and P. F. M. Verdonschot, Effect-based nationwide surface water quality assessment to identify ecotoxicological risks, *Water Res.*, 2019, **159**, 434–443.

30 C. R. IBM, *IBM SPSS Statistics for Windows, Version 24.0*, IBM Corp, Armonk, NY, 2016.

31 L. Haanstra, P. Doelman and J. H. O. Voshaar, The use of sigmoidal dose-response curves in soil ecotoxicological research, *Plant Soil*, 1985, **84**, 293–297.

32 S. J. Klaine, G. P. Cobb, R. L. Dickerson, K. R. Dixon, R. J. Kendall, E. E. Smith and K. R. Solomon, An ecological risk assessment for the use of the biocide dibromonitrilopropionamide (DBNPA) in industrial cooling systems, *Environ. Toxicol. Chem.*, 1996, **15**, 21–30.

33 A. J. Sumner and D. J. Plata, Halogenation chemistry of hydraulic fracturing additives under highly saline simulated subsurface conditions, *Environ. Sci. Technol.*, 2018, **52**, 9097–9107.

34 G. A. Kahrilas, J. Blotevogel, P. S. Stewart and T. Borch, T. Biocides in hydraulic fracturing fluids: A critical review of their usage, mobility, degradation, and toxicity, *Environ. Sci. Technol.*, 2015, **49**, 16–32.

35 G. Ganzer, J. Summerfield, M. Freid, J. Soost and G. Regginni, *The use of glutaraldehyde/DBNPA combination treatment program for effective control of microbial growth in cooling water systems*, Corrosion 2002, NACE International.

36 E. P. A. US, *Reregistration eligibility decision (RED), 2,2-dibromo-3-nitrilopropionamide (DBNPA)*, United States Environmental Protection Agency, 1994.

37 F. Cheng, The chronic aquatic toxicity of a microbiocide dibromonitrilopropionamide, *Toxicol. Ind. Health*, 2011, **28**, 181–185.

38 T. V. Wagner, V. de Wilde, B. Willemsen, M. Mutaqin, G. Putri, J. Opdam, J. R. Parsons, H. H. M. Rijnaarts, P. de Voogt and A. A. M. Langenhoff, Pilot-scale hybrid constructed wetlands for the treatment of cooling tower water prior to desalination, *J. Environ. Manage.*, submitted.

